ISSN 0023-1584, Kinetics and Catalysis, 2010, Vol. 51, No. 3, pp. 428–437. © Pleiades Publishing, Ltd., 2010.
Original Russian Text © V.A. Matyshak, O.N. Sil'chenkova, I.T. Ismailov, V.F. Tret'yakov, 2010, published in Kinetika i Kataliz, 2010, Vol. 51, No. 3, pp. 447–456.

Mechanism of Methanol Conversion on ZrO_2 and 5% Cu/ZrO_2 According to In Situ IR Spectroscopic Data

V. A. Matyshak[a], O. N. Sil'chenkova[a], I. T. Ismailov[b], and V. F. Tret'yakov[b]

[a] *Semenov Institute of Chemical Physics, Russian Academy of Sciences, Moscow, 119991 Russia*
[b] *Topchiev Institute of Petrochemical Synthesis, Russian Academy of Sciences, 119991 Russia*
e-mail: matyshak@polymer.chph.ras.ru

Received September 7, 2009

Abstract—It is demonstrated by in situ IR spectroscopy that, in methanol conversion on ZrO_2 and 5% Cu/ZrO_2 catalysts, methoxy groups are present on the catalyst surface, which result from O–H or C–O bond breaking in the methanol molecule. Two types of formate complexes, localized on ZrO_2 and CuO, are also observed. The formate complexes form via the oxidative conversion of the methoxy groups. There are two types of linear methoxy groups. First-type linear methoxy groups condense with the formate complex located on CuO to yield methyl formate and then CO and H_2. Second-type methoxy groups appear as intermediate products in the formation of dimethyl ether. The main hydrogen formation reactions are the recombination of hydrogen atoms (which result from the interconversion of surface complexes) on copper clusters and the decomposition of methyl formate. The source of CO_2 in the gas phase is the formate complex, and the source of CO is methyl formate. The effect of water vapor and oxygen the surface reactions and product formation is discussed.

DOI: 10.1134/S002315841003016X

INTRODUCTION

In recent years, much attention has been focused on obtaining H_2-containing gas mixtures from methanol. This is largely due to the development of hydrogen fuel cells. Hydrogen-rich mixtures can be obtained by the catalytic decomposition and steam and autothermal reforming of methanol [1–4]. Obviously, information concerning the mechanism of surface reactions would be helpful in the design of efficient methanol decomposition catalysts.

As follows from the literature [5–9], the interaction of methanol with oxide catalysts typically yields methoxy groups and formate, aldehyde, and carbonate complexes on the catalyst surface. However, the role of these complexes in the formation of products, such as carbon monoxide and dioxide and hydrogen, has not been elucidated, apparently because there has been no comparison between the surface complex conversion and product formation rates.

Earlier, we studied methanol conversion on CeO_2 and 5% CuO/CeO_2 catalysts by in situ IR spectroscopy [10]. Formate and carbonate complexes and bridging and linear methoxy groups were identified on the surface of these catalysts, and the reaction products were H_2, methyl formate (MF), CO, CO_2, and H_2O.

This earlier study demonstrated that hydrogen results mainly from the recombination of hydrogen atoms on copper clusters and from MF decomposition. The sources of CO_2 in the gas phase are the formate and carbonate complexes, and the source of CO is MF. The introduction of water vapor into the reacting stream exerts a favorable effect on the outcomes of the reaction, reducing the CO formation rate without changing the hydrogen yield.

Here, we report a similar study of the role of surface complexes in methanol conversion for copper-containing catalysts supported on ZrO_2.

EXPERIMENTAL

Zirconium dioxide was synthesized via a standard procedure [11]. According to X-ray diffraction data, the resulting zirconia was a mixture of monoclinic (m-ZrO_2) and tetragonal (t-ZrO_2) phases. Its specific surface area was 116 m^2/g. The sample containing 5% copper was prepared by impregnating zirconia with a copper nitrate solution followed by drying at 100°C and calcination at 500°C in air for 2 h.

The state of copper in the catalyst was characterized by CO adsorption from the 1% CO + He mixture, temperature-programmed reduction (TPR), and diffuse reflectance spectroscopy. The spectra of powder samples were recorded on a Hitachi 330 spectrophotometer.

The feed gas was composed of 14% methanol, helium, and up to 3% oxygen. Helium contained 0.2% oxygen as an impurity.

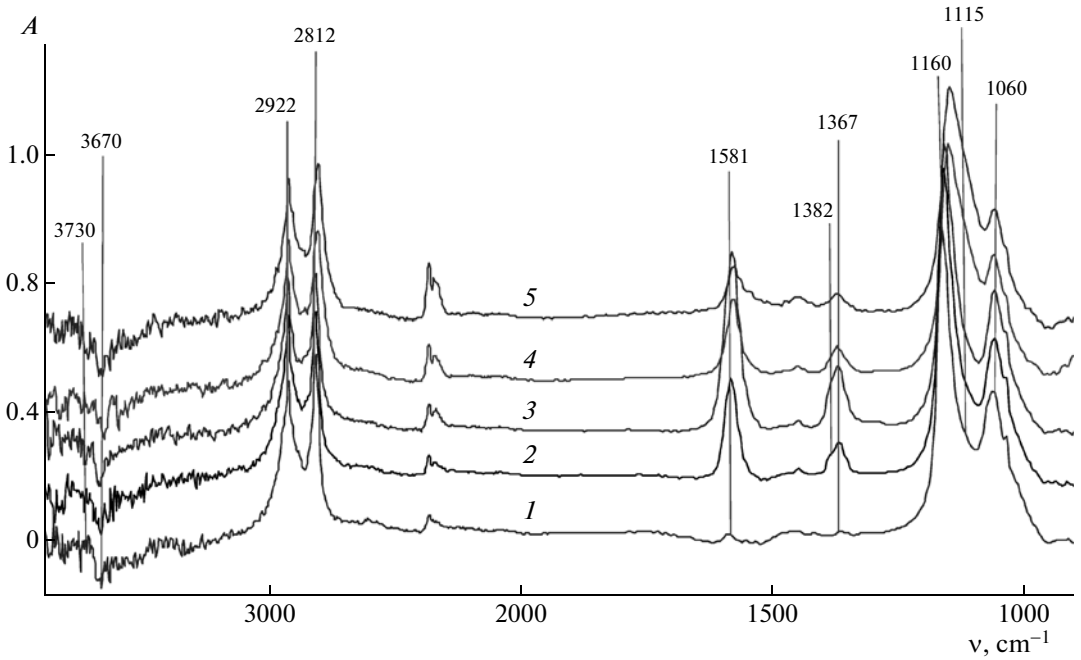

Fig. 1. IR spectra recorded for methanol (14 vol % MeOH + He) decomposition on ZrO_2 at $T = (1)$ 180, (2) 242, (3) 280, (4) 347, and (5) 375°C.

Spectrokinetic measurements under methanol conversion conditions are described elsewhere [12].

The experimental setup included a Bruker IFS 45 FTIR spectrometer, a heated 1-cm^3 reactor cell, a gas preparation unit, and a product and reactant analysis system. The sample as a 20- to 30-mg pellet with a surface area of 2 cm^2 was placed in the cell, which also served as a catalytic flow reactor. Prior to measurements, the sample was heat-treated at 450°C in flowing He for 1 h and was then cooled to the preset temperature. Thereafter, the reaction mixture was passed through the cell at a rate of 30 ml/min.

In unsteady-state spectrokinetic experiments, we measured the concentration of surface species by in situ IR spectroscopy as the methanol conversion reaction was coming to a steady state or after the elimination of methanol from the feed.

The intensity of absorption bands was measured in difference spectra in units of absorbance (A). These spectra were obtained by subtracting, from the spectrum of the sample in flowing reaction mixture, the spectrum of the same sample in flowing inert gas at the same temperature. The number of coadditions was usually 64, and the spectral resolution was 4 cm^{-1}.

Reactant and product concentrations were measured on a Model 3700 chromatograph with heated pipelines using helium as the carrier gas. Dimethyl ether (DME), methanol, and methane were identified using a Porapak Q column and a flame-ionization detector. CO, H_2, and CO_2 were quantified using molecular sieve 5A and Porapak Q columns and a thermal-conductivity detector.

RESULTS

ZrO_2

Steady-state measurements. Figure 1 shows the difference IR spectra recorded under the methanol (4% MeOH in He) conversion conditions. The spectra show absorption bands in the region of C–O vibrations in the linear methoxy groups (1160 and 1120 cm^{-1}) and in the bridging one (1060 cm^{-1}) [13–16] and bands due to the monodentate formate complex (1580, 1382, and 1367 cm^{-1}) [17]. In the 2800–3000 cm^{-1} range, there are a number of absorption bands due to C–H stretching vibrations in the methoxy groups and formate complex [13–17]. The methoxy group and formate vibration frequencies decrease as the reaction temperature is raised.

Negative absorbance with peaks at 3670 and 3730 cm^{-1} is observed in the region of the stretching vibrations of surface OH groups (Fig. 1). These negative band intensities in the difference spectra indicate that surface hydroxyl groups disappear in the interaction between methanol and the catalyst surface.

Figure 2 plots the temperature dependences of the concentrations of methanol and its conversion products and those of band intensities measured in the same run. Clearly, H_2, CO, DME, and CH_4 formation takes place only above 300°C (Fig. 2b). The weaken-

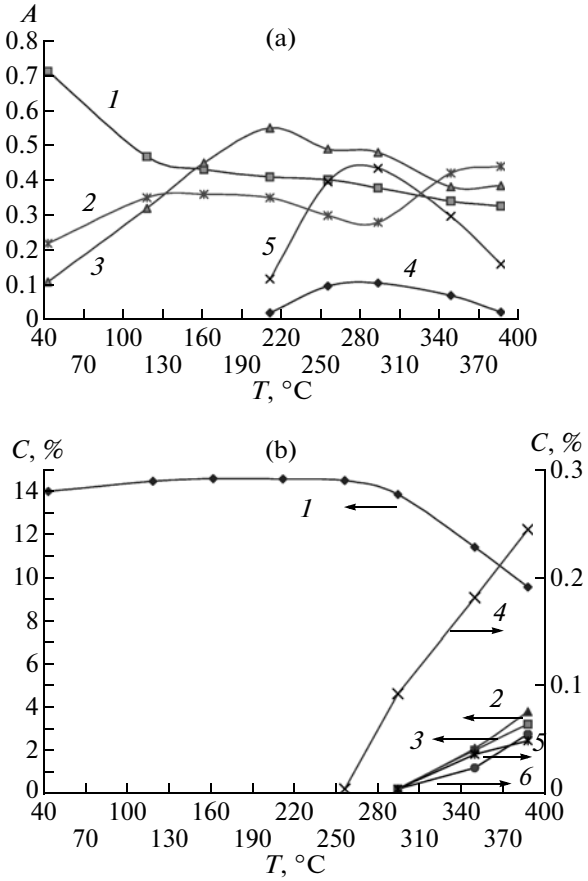

Fig. 2. Temperature dependences of the (a) intensities of the absorption bands of surface compounds and (b) product concentrations for methanol decomposition on ZrO_2: (a) ν = (*1*) 1060, (*2*) 1120, (*3*) 1160, (*4*) 1380, and (*5*) 1581 cm^{-1}; (b) (*1*) CH_3OH, (*2*) H_2, (*3*) CO, (*4*) CO_2, (*5*) CH_4, and (*6*) DME.

ing of the absorption bands of the methoxy groups (Fig. 2a, curves *1*–*3*) in the 190–280°C range is accompanied by the strengthening of the bands of the formate complexes (curves *4*, *5*). The weakening of the bands of the formate complexes and methoxy groups is accompanied by an increase in the product concentrations (Fig. 2).

Unsteady-state measurements. After the establishment of a steady-state concentration of surface compounds under the 14% MeOH + He flow, methanol was eliminated from the feed and the surface compounds were desorbed isothermally into the helium flow. The intensities of the IR absorption bands of the surface compounds were monitored in the 150–350°C range.

The kinetic curves obtained in this way allowed the kinetic order of the surface complex disappearance process and the effective rate constants to be determined. The equation describing the time variation of the methoxy group concentration is first-order. Table 1 lists temperature-dependent methoxy group disappearance rate constants.

The kinetic curves for formate formation on the surface at low temperatures were also processed in the coordinates of a first-order equation. The formate formation rate constants are presented in Table 1. As the temperature is raised, a maximum appears in the formate concentration versus time curve. This means that both the formation and disappearance of the formate complexes take place at elevated temperatures.

It is clear from the data presented in Table 1 that the sum of the methoxy group disappearance rate constants at 21°C us close to monodentate formate formation rate constant (absorption band at 1580 cm^{-1}). Note also that the methoxy group disappearance rate constants increase sharply on passing from 290 to 346°C owing to the high rate of the reaction at 346°C (Fig. 2b).

5% Cu/ZrO₂

The same surface complexes, but with somewhat different vibration frequencies, are observed for the copper oxide–containing catalyst. A shape analysis of the absorption band of the formate complex on the 5% Cu/ZrO_2 surface demonstrated that, along with the complex described for ZrO_2, there is another one on

Table 1. Rate constants of methoxy group disappearance and formate formation in methanol conversion on ZrO_2

T, °C	Rate constant, min^{-1} ($n = 1$)				
	methoxy group disappearance			formate formation	formate disappearance
	Absorption bands				
	1060 cm^{-1}	1120 cm^{-1}	1160 cm^{-1}	1580 cm^{-1}	
145	0.012	0.16	0.014	0	–
210	0.021	0.025	0.023	0.065	–
290	0.027	0.028	0.032	–	–
346	0.148	0.152	0.176	–	0.070

this sample, which shows itself at 1595 cm^{-1}. Since this species is observed only in the presence of copper, it is natural to assume that it is localized on copper oxide clusters.

Figure 3 plots the concentrations of MeOH and reaction products (H_2, MF, CO, CO_2, and CH_4) and band intensities as a function of temperature. Clearly, the reaction over the copper-containing catalyst yields a different product composition: MF is observed here. In addition, the reaction products form at lower temperatures and their concentrations are considerably higher than in the case of ZrO_2 (Figs. 2b, 3b). It is interesting that, on passing from 250 to 300°C, the outlet methanol concentration somewhat increases (Fig. 3b, curve *1*), while the H_2 and CO_2 concentrations decrease (curves *2* and *4*, respectively). This fact can be explained by the occurrence of the reverse reaction (methanol synthesis from H_2 and CO_2) in this temperature interval. A similar effect was observed for CeO_2-supported catalysts [18]. Note that the formation of H_2, CO_2, and MF (curves *2*, *4*, *6*) begins at a lower temperature than the formation of CO, CH_4, and DME (curves *3*, *5*, *7*).

Figure 3a shows the temperature dependences of band intensities measured for the surface compounds in the same run. As the temperature is raised, the concentration of linear methoxy groups with a vibration frequency of 1160 cm^{-1} passes through a maximum at 300°C, the concentration of bridging methoxy groups decreases steadily, and the concentration of linear methoxy groups with a vibration frequency of 1120 cm^{-1} increases (Fig. 3a, curve *2*). The formate concentration passes through a maximum at 200°C and begins to increase again above 300°C (Fig. 3a, curve *5*). This increase concurs with the decrease in the concentration of linear methoxy groups with a vibration frequency of 1160 cm^{-1} (curve *3*).

An analysis of the spectroscopic and catalytic data (Figs. 3a, 3b) suggests that product formation takes place in the same temperature range as the conversion of the formate complexes and methoxy groups.

Effects of water vapor and oxygen. Figure 4 presents the temperature dependences of the MeOH and product concentrations and band intensities obtained under the methanol conversion condition in the presence of various concentrations of water vapor. The introduction of water vapor into the system in the temperature range of the reaction decreases the intensity and frequency of the linear methoxy group band at 1160 cm^{-1} (Fig. 4d, curves *1*, *2*). In addition, water vapor increases the intensity of the formate band at 1580 cm^{-1} (Fig. 4d, curves *3*, *4*). The position and intensity of the linear methoxy group band at 1120 cm^{-1} and those of the bridging methoxy group band at 1060 cm^{-1} change only slightly. The temperature dependences of the intensities of these bands were discussed above (Fig. 3).

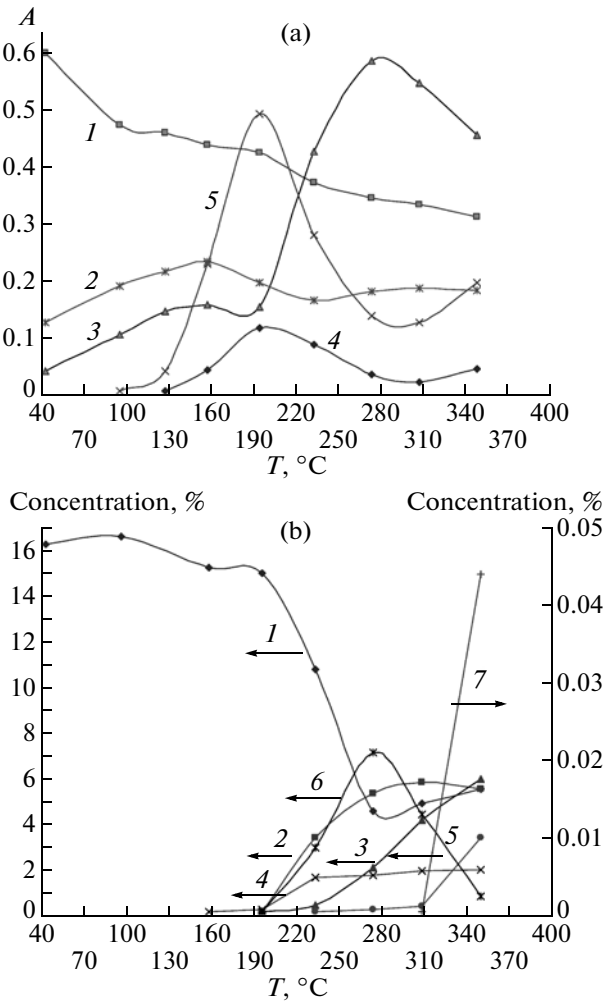

Fig. 3. Temperature dependences of the (a) intensities of the absorption bands of surface compounds and (b) product concentrations for methanol decomposition on 5% Cu/ZrO_2: (a) ν = (*1*) 1060, (*2*) 1120, (*3*) 1160, (*4*) 1380, and (*5*) 1581 cm^{-1}; (b) (*1*) CH_3OH, (*2*) H_2, (*3*) CO, (*4*) CO_2, (*5*) CH_4, (*6*) MF, and (*7*) DME.

In the presence of water vapor, the H_2 concentration remains practically invariable (Fig. 4a), the concentrations of CO (Fig. 4b) and methane (Fig. 4c) are somewhat lower, and the CO_2 concentration (Fig. 4b) is higher. Under the action of water vapor, MF formation stops (Fig. 4a) and the DME concentration decreases markedly (Fig. 4c, curves *3*, *4*).

Figure 5 plots the same temperature dependences recorded under methanol conversion conditions in the presence of various amounts of oxygen. Oxygen also decreases the concentration of linear methoxy groups (1160 cm^{-1}) and increases the formate concentration (Fig. 5d) over the temperature range of the reaction. It increases the CO_2 formation rate and reduces the formation rates of CO, MF (Fig. 5b), CH_4, and DME (Fig. 5c). These data indicate that water vapor and oxygen exert similar effects on the reaction.

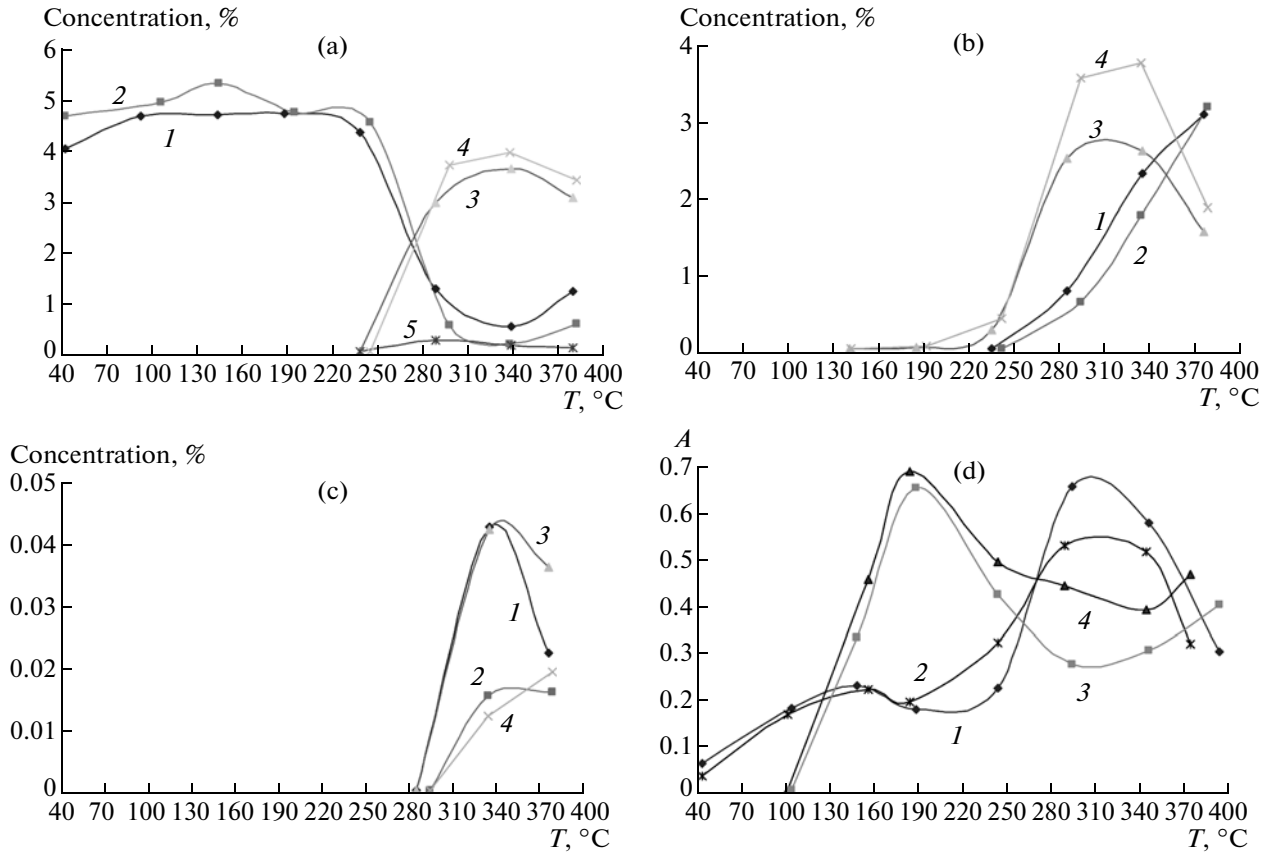

Fig. 4. Temperature dependences of (a–c) product concentrations and (d) absorption band intensities for methanol (14 vol % MeOH + He) decomposition on 5% Cu/ZrO_2 at water vapor concentrations of (*1*, *3*, *5*) 0 and (*2*, *4*) 3%: (a) (*1*, *2*) CH_3OH, (*3*, *4*) H_2, and (*5*) MF; (b) (*1*, *2*) CO and (*3*, *4*) CO_2; (c) (*1*, *2*) methane and (*3*, *4*) DME; (d) (*1*, *2*) methoxy groups (1160 cm^{-1}) and (*3*, *4*) formate structures (1580 cm^{-1}).

Unsteady-state measurements. The time dependences of the methoxy group band intensities for isothermal desorption (below 250°C) can be fitted to a first-order equation. At 250°C and higher temperatures, the methoxy group conversion rate increases considerably and these dependences obey a second-order equation. Examples of the linear fit of the time dependence of band intensity to a second-order equation are given in Fig. 6. The rate constants of the corresponding processes are listed in Table 2.

Table 2. Rate constants of the conversion of surface compounds in methanol conversion on 5% Cu/ZrO_2

Surface compound	Frequency, cm^{-1}	Rate constants of the conversion of surface compounds, min^{-1}						
		$n = 1$			*$n = 2$			
T, °C		140	170	210	250	250 (H_2O)	250 (O_2)	340
Methoxy group	1155	0.026	0.035	0.057	11.45	18.78	24.91	–
	1115	0.024	0.038	0.064	7.69	8.50	19.68	–
	1055	0.024	0.040	0.059	2.73	3.12	5.01	–
		$n = 1$						
Formate	1580	–	–	–	0.0838	0.074	0.090	0.35
		Rate constant of formate formation, min^{-1}						
		0.066	–	–	–	–	–	–

* The rate constants were determined spectroscopically, using concentrations estimated from absorbance (*A*) data.

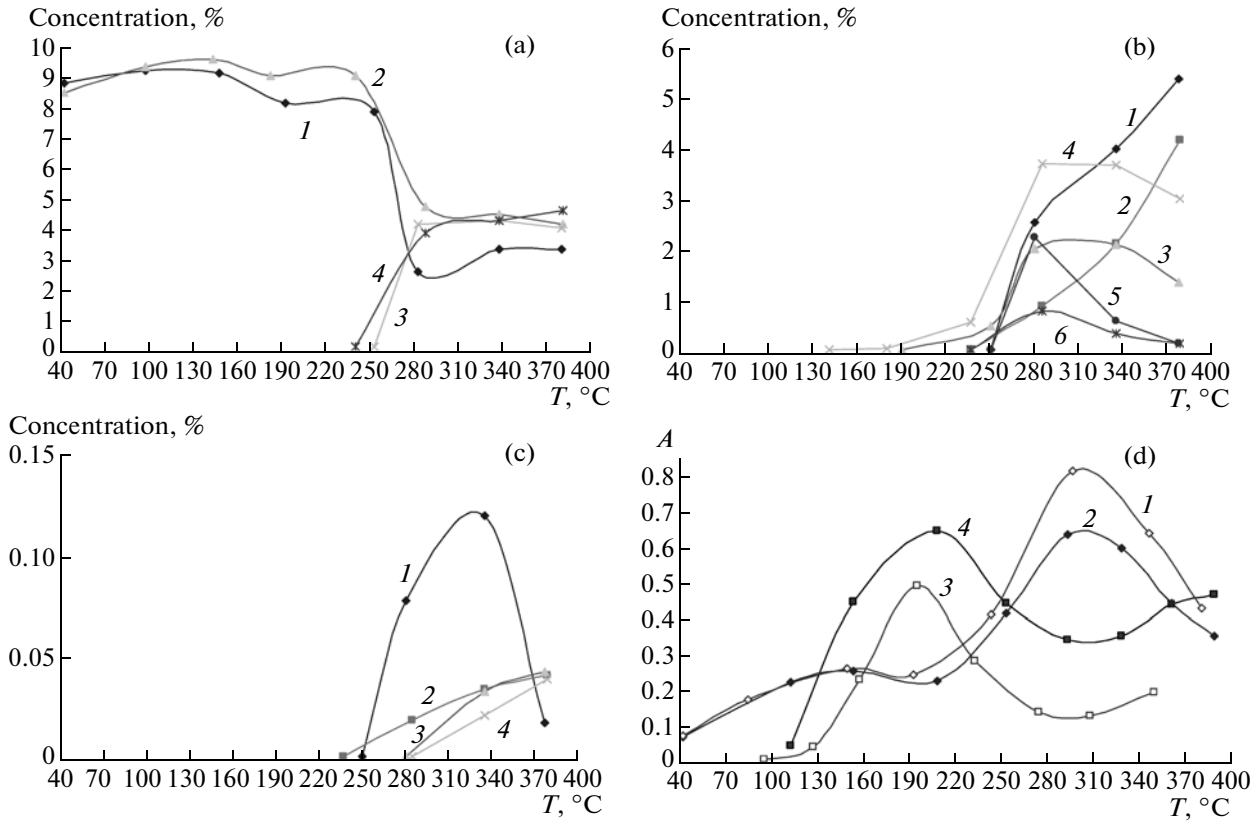

Fig. 5. Temperature dependences of (a–c) product concentrations and (d) absorption band intensities for methanol (14 vol % MeOH + He) decomposition on 5% Cu/ZrO_2 at oxygen concentrations of (*1*, *3*, *5*) 0 and (*2*, *4*, *6*) 3%: (a) (*1*, *2*) CH_3OH, (*3*, *4*) H_2; (b) (*1*, *2*) CO and (*3*, *4*) CO_2, and (*5*, *6*) MF; (c) (*1*, *2*) methane and (*3*, *4*) DME; (d) (*1*, *2*) methoxy groups (1160 cm^{-1}) and (*3*, *4*) formate structures (1580 cm^{-1}).

The introduction of water vapor into the reaction system at 250°C increases the disappearance rate constants of the linear methoxy groups, and a still stronger effect is produced by oxygen (Table 2). The disappearance rate constant of the bridging methoxy group is less sensitive to the presence of water vapor and to an increase in the oxygen concentration. As was reported above, the MF and DME formation rates decrease under the action of oxygen and water vapor (Figs. 4, 5).

The conversion of the formate complex obeys a first-order equation with a rate constant almost independent of the presence of water vapor and oxygen (Table 2).

DISCUSSION

Model of the Active Surface

The diffuse reflectance spectrum of 5% Cu/ZrO_2 (Fig. 7) shows a charge transfer band at 36360 cm^{-1} and *d–d* transition bands at 12500 cm^{-1} ($^2B_{1g} \rightarrow {}^2B_{2g}$ and $^2B_{1g} \rightarrow {}^2E_g$) and 5200 cm^{-1} ($^2B_{1g} \rightarrow {}^2A_{1g}$). This spectrum was attributed to isolated Cu^{2+} ions with an octahedral, tetragonally distorted coordination sphere [19] (large copper oxide particles are unobservable by diffuse reflectance spectroscopy because of exchange interactions). As was found by TPR, copper oxide in this sample is in two states, undergoing reduction at 130 and 200°C. According to the literature [19, 20],

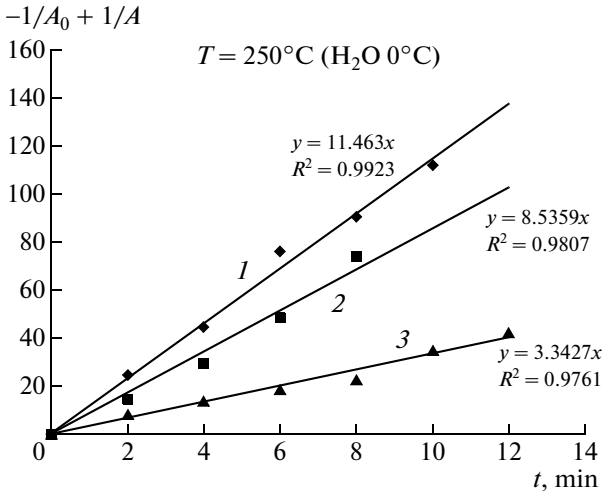

Fig. 6. Time dependences of the intensities of the absorption bands of the methoxy groups in the coordinates of the second-order equation for 5% Cu/ZrO_2 at 250°C: ν = (*1*) 1150, (*2*) 1110, and (*3*) 1074 cm^{-1}.

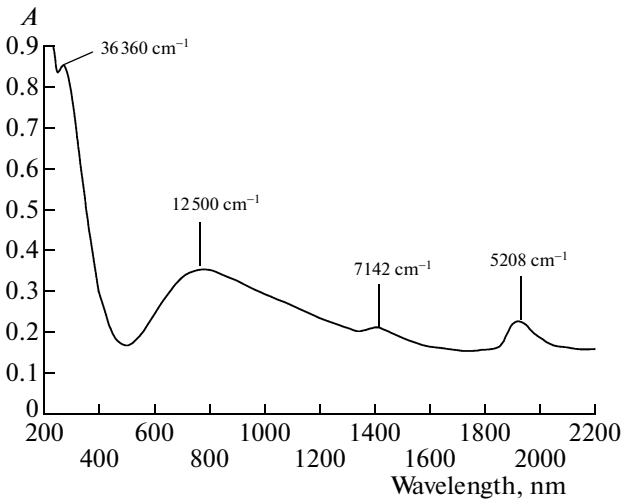

Fig. 7. Diffuse reflectance spectrum of 5% Cu/ZrO_2.

these states may correspond to finely dispersed and clustered copper ions. The totality of the data presented here demonstrates that the copper oxide in the copper-containing catalyst is just in these two states—finely divided and clustered. It is interesting that the IR spectrum of adsorbed CO molecules (40–170°C) exhibits an absorption band at 2100 cm^{-1}, which is due to vibrations in the Cu^0–CO complex [18, 19]. This can be explained by the fact that, in the presence of CO, the finely dispersed copper ions undergo reduction even at 40°C. The ease of their reduction is evidently due to the coordination sphere of Cu^{2+} having anionic vacancies [20, 21] occupied by active forms of atomic oxygen. The existence of this kind of sites on the surface was proved by experiments on the isothermal desorption of surface compounds (after the elimination of methanol from the feed). For ZrO_2 and 5% Cu/ZrO_2, we observed a bathochromic shift of the absorption bands of the methoxy groups in time. This was reported to be due to the oxidation of the surface [14, 15]. Indeed, in the presence of methanol, active oxygen in the anionic vacancies is spent for methanol oxidation, as is indicated by the appearance of CO_2 in the gas phase (Fig. 2). As a result, the surface undergoes reduction. (Data concerning copper oxide reduction in the presence of methanol are presented in [22].) After methanol elimination from the feed, the anionic vacancies are occupied by oxygen present in the carrier gas as an impurity and the surface is thus oxidized.

Conversion of Surface Compounds

The data reported for methoxy groups on the ZrO_2 surface are controversial. Alekseev et al. [13], who studied the interaction of methanol with hydroxyl groups on the ZrO_2 surface, identified linear (1170 cm^{-1}) and bridging (1060 cm^{-1}) methoxy groups. Bianci et al. [16] described a single type of methoxy group (1144 cm^{-1}). Other authors [14, 15, 23] reported linear (1163 cm^{-1}) and bridging (1056 cm^{-1}) methoxy groups resulting from the interaction of methanol with coordinatively unsaturated Zr^{4+} ions. In the latter case, the absorption band of the bridging methoxy group is broadened on its high-frequency side, so that a band due to another kind of methoxy group can be distinguished near 1100 cm^{-1}. These discrepancies arise from the variation of the phase composition of the zirconia samples. It was demonstrated that two types of methoxy groups occur on the surface of monoclinic zirconia and only one type is observed for the tetragonal modification [24]. This is confirmed by the observation of two methoxy group vibration frequencies—1155 and 1051 cm^{-1}—for monoclinic ZrO_2 [25]. Our sample consisted of the tetragonal and monoclinic phases in approximately equal proportions. In view of the above, it is evident that the linear and bridging methoxy groups with vibration frequencies of 1160 and 1056 cm^{-1}, respectively, are localized in the monoclinic phase. The other type of linear methoxy group (1115 cm^{-1}) is localized in the tetragonal phase.

The following three mechanisms of methoxy group formation were described in the literature (see, e.g., [26]): C–O bond breaking in the methanol molecule involving acidic hydroxyl groups of the surface; O–H bond breaking in the methanol molecule involving basic hydroxyl groups of the surface; and methanol adsorption on coordinatively unsaturated metal ions, which yields hydroxyl groups. In our case, negative absorbance with maxima at 3670 and 3730 cm^{-1} is observed in the region of the stretching vibrations of surface OH groups (Fig. 1). The OH groups with such vibration frequencies are localized in the monoclinic and tetragonal phases, respectively [24]. The negative absorbances in the difference spectra (Fig. 1b) suggest that these hydroxyl groups, characterized by acid and base properties, are involved in the formation of methoxy groups vibrating at 1056 and 1115 cm^{-1}. In addition, as follows from the data presented in Figs. 2–5, the concentration of methoxy groups with the vibration frequency 1160 cm^{-1} increases as the temperature is raised to 300°C. Since the number of hydroxyl groups on the surface decreases and the number of coordinatively unsaturated Zr^{4+} sites increases with increasing temperature, it is believed that this type of methoxy group results from methanol binding to the coordinatively unsaturated Zr^{4+} ions. Thus, all of the three methoxy group formation mechanisms take place on the 5% Cu/ZrO_2 surface.

The IR spectra recorded for the ZrO_2-catalyzed reaction (Fig. 1) show absorption bands at 1580, 1367, and 1382 cm^{-1}, which are due to vibrations in the surface formate complex (see, e.g., [26–30]). A shape analysis of the bands of the formate complex on 5% Cu/ZrO_2 (Fig. 3) demonstrated that, along with this complex, there is another formate complex, charac-

terized by a vibration frequency of 1595 cm^{-1}, on the surface of this sample. Since this shape of absorption band is observed only in the presence of copper, this complex is likely localized on copper oxide clusters.

The weakening of the absorption bands of the methoxy groups with time in isothermal desorption from ZrO_2 obeys a first-order equation. As follows from the data presented in Fig. 2, no reaction products or surface compounds form at 145°C. In this case, the weakening of the bands of methoxy groups with time indicates that the main methoxy group conversion route is desorption and methanol formation in the gas phase [16]. However, as the temperature is raised, the methoxy groups begin to participate in formate formation in addition to being desorbed. The marked increase in the methoxy group disappearance rate constants at 350°C (Table 1) is due to methanol conversion into a hydrogen-cont6aining gas mixture occurring at a noticeable rate (Fig. 2).

The expression for the methoxy group conversion rate is written as follows [10]:

$$d(CH_3OZ)/dt = -\theta_{CH_3OZ}(k_3\theta_O + k_7\theta_{ZH}). \quad (1)$$

Here, k_3 and k_7 are the rate constants of formate complex formation and methoxy group desorption, respectively.

The oxygen coverage of the surface is constant (θ_O = const) because impurity oxygen (up to 0.2%) is always present in the gas stream, and the H or hydroxyl coverage of the surface changes insignificantly during desorption. This is why the methoxy group concentration varies according to a first-order equation. The rate constants for different methoxy groups are fairly similar (Table 1), and it is, therefore, impossible to identify the type of methoxy group responsible for formate formation. However, based on the rate constant ratios at 210°C and Eq. (1), it can be deduced that all of the three types of methoxy groups are involved in formate formation and that the contribution from desorption to the disappearance of methoxy groups at this temperature is small.

This is also true for the 5% Cu/ZrO_2 catalyst up to 210°C (Table 2). At 250°C, the methoxy group conversion in the efficient reaction zone passes from the first- to the second-order rate law (Fig. 6). The expression for the methoxy group conversion rate in this case appears as

$$d(CH_3OZ)/dt = -\theta_{CH_3OZ}(k_3\theta_O + k_4\theta_F + k_7\theta_{ZH}). \quad (2)$$

Here, k_4 is the MF formation rate constant and θ_F is the formate coverage of the surface. The second order of methoxy group disappearance is likely due to the fact that the main contribution to the right-hand side of Eq. (2) is from the $k_4\theta_F$ term (MF formation rate).

As follows from our earlier data [10, 31, 32], the following two conditions are necessary for MF formation: the presence of the formate complex localized on copper clusters and the presence of a linear methoxy group that has resulted from the interaction of a methanol molecule with a basic hydroxyl group or a coordinatively unsaturated site (in other words, O–H bond breaking in the methanol molecule). Both of these conditions are satisfied with the 5% Cu/ZrO_2 catalyst, as distinct from ZrO_2. As a consequence, MF forms only over the copper-containing catalyst. MF formation as a result of condensation between the formate complex and a methoxy group was also reported by other authors [28–30].

According to our earlier studies [10, 31, 32], DME results from the recombination of bridging methoxy groups. The fact that only traces of DME form on ZrO_2 and 5% Cu/ZrO_2 (Figs. 2, 6) and that water vapor slows down DME formation (Fig. 4) suggests that the diffusion of bridging methoxy groups on the catalysts is hampered.

As the temperature is raised, the MF concentration decreases (Fig. 5b) because of MF decomposition to H_2 and CO. Another source of hydrogen (and CO_2) in the case of 5% Cu/ZrO_2 is the conversion of the formate complex. This is indicated by the fact that the simultaneous appearance of CO_2 and hydrogen in the gas phase takes place at the same temperature as the decrease in the formate concentration on the surface (Figs. 3–5).

In brief, the most significant surface reactions occurring in methanol conversion can be written as follows (a more detailed reaction network is presented elsewhere [10]):

$$CH_3OZ + ZO \rightarrow HCOOZ + Z + H_2,$$
$$CH_3OZ + HCOOZ \rightarrow HCOOCH_3Z + ZO,$$
$$HCOOCH_3Z \rightarrow 2CO + 2H_2 + Z,$$
$$HCOOZ \rightarrow CO_{2(g)} + ZH,$$
$$ZH + ZH \rightarrow H_{2(g)} + 2Z.$$

In addition, deep methanol oxidation takes place on ZrO_2 in the presence of oxygen in the reaction mixture. This is indicated by the fact that CO_2 is the only reaction product at comparatively low temperatures (Fig. 2). The oxidizing power of surface oxygen is obviously due to the oxygen species occupying anionic vacancies.

Role of Cu in Methanol Conversion on 5% Cu/ZrO_2

The presence of copper in the catalyst significantly enhances its activity and changes the product composition, while the composition of the surface complexes remains nearly the same (Figs. 2, 3). Therefore, new surface reactions between the same complexes become possible in the presence of copper. The most important of these reactions are hydrogen atom recombination on copper clusters (hydrogen atoms result from the interconversion of surface compounds, such as $HCOOZ \rightarrow CO_2(g) + ZH$ [5]) and the reaction between the linear methoxy group and the formate complex located on copper, which yields MF. Thus, there are two main hydrogen formation routes—

hydrogen atom recombination on copper oxide particles and MF decomposition ($W_{H_2} = k_7\theta_{MF} + k_{13}\theta_H^2$).

The decrease in the formation and disappearance temperatures of the surface formate complexes suggests that copper markedly raises the oxidizing power of the catalyst. This property of the catalyst is due to oxygen activation on supported copper.

It is interesting that the introduction of oxygen and water vapor decreases the MF and DME formation rates (Figs. 4, 5). According to spectroscopic data, the introduction of oxygen and water vapor diminishes the concentration of linear methoxy groups (1160 cm^{-1}) and increases the concentration of formate complexes (Figs. 4d, 5d). Apparently, surface oxidation takes place when water vapor and oxygen are present simultaneously. Oxidation (increase in the surface oxygen concentration) changes both the state of copper particles and the state of the copper-modified ZrO_2 surface (the oxidation of surface Cu^0 or Cu^{+1} with water was demonstrated in [33–35]). On the oxidized surface, the oxidative conversion of methoxy groups dominates over the condensation of methoxy groups with formate complexes.

Comparison with CeO_2

A bridging methoxy group, a linear one, and formate and carbonate complexes exist on the CeO_2 and 5% Cu/CeO_2 surfaces under methanol conversion conditions. CO, CO_2, H_2, CH_4, and MF were detected among the reaction products. A bridging methoxy group, two types of linear methoxy groups, and a formate complex were identified on the ZrO_2 and Cu/ZrO_2 surfaces under the same conditions. DME was detected among the reaction products along with above compounds. The difference between the product compositions can be explained in terms of the methoxy group formation mechanism. On 5% Cu/CeO_2, the methoxy groups result from the interaction between methanol and basic hydroxyl groups with O–H bond breaking in the alcohol molecule; on 5% Cu/ZrO_2, their formation involves both basic hydroxyl groups (O–H bond breaking) and acidic ones (C–O bond breaking in the alcohol molecule). The first-type linear methoxy groups condense with the formate complex to yield MF and then CO and H_2. The second-type linear methoxy groups are intermediates in DME formation.

From the standpoint of obtaining hydrogen-containing gas mixtures from methanol, MF formation is an undesired process because MF decomposition yields not only H_2, but also CO, which is poisonous to the electrodes of the fuel cell. In this case, it is appropriate to introduce water vapor and oxygen into the feed: this will significantly reduce the CO formation rate and prevent MF formation without affecting the hydrogen yield. The addition of oxygen and water vapor leads to surface oxidation. On this oxidized surface, the oxidative conversion of methoxy groups into CO_2 and H_2 via formate dominates over methoxy group–formate condensation.

CONCLUSIONS

The above analysis demonstrates that the main hydrogen formation reactions are hydrogen atom recombination on copper clusters and MF decomposition, and the source of CO is MF. It is appropriate to introduce oxygen and water vapor into the feed: this will decrease the CO formation rate without affecting the hydrogen yield.

ACKNOWLEDGMENTS

This work was support by the Russian Foundation for Basic Research, grant no. 07-03-00373.

REFERENCES

1. Lindström, B., Pettersson, L., and Menon, P.G., *Appl. Catal., A*, 2002, vol. 234, p. 111.
2. Zhang, X. and Shi, P., *J. Mol. Catal. A: Chem.*, 2003, vol. 194, p. 99.
3. Iwasa, N., Mayanagi, T., and Ogawa, N., *Catal. Lett.*, 1998, vol. 54, p. 119.
4. Kapoor, M.P., Raj, A., and Matsumura, Y., *Microporous Mesoporous Mater.*, 2001, vol. 44, p. 565.
5. Schiffino, R.S. and Merril, R.P., *J. Phys. Chem.*, 1993, vol. 97, p. 6425.
6. Krylov, O.V. and Matyshak, V.A., *Promezhutochnye soedineniya v geterogennom katalize* (Intermediates in Heterogeneous Catalysis), Moscow: Nauka, 1996.
7. Matyshak, V.A., Khomenko, T.I., Lin, G.I., Zavalishin, I.N., and Rozovskii, A.Ya., *Kinet. Katal.*, 1999, vol. 40, no. 2, p. 295 [*Kinet. Catal.* (Engl. Transl.), vol. 40, no. 2, p. 269].
8. Neophytides, S.G., Marchi, A.J., and Froment, G.F., *Appl. Catal., A*, 1992, vol. 86, p. 45.
9. Martin, K.A. and Zabransky, R.F., *Appl. Spectrosc.*, 1991, vol. 45, p. 68.
10. Matyshak, V.A., Sil'chenkova, O.N., Ismailov, I.T., and Tret'yakov, V.F., *Kinet. Katal.*, 2009, vol. 50, no. 5, p. 816 [*Kinet. Catal.* (Engl. Transl.), vol. 50, no. 5, p. 784].
11. Chuah, G.K., *Catal. Today*, 1999, vol. 49, p. 131.
12. Matyshak, V.A. and Krylov, O.V., *Catal. Today*, 1996, vol. 25, p. 1.
13. Alekseev, A.V., Lopatin, Yu.N., Tsyganenko, A.A., and Filimonov, V.N., *React. Kinet. Catal. Lett.*, 1974, vol. 1, no. 4, p. 443.
14. Daturi, M., Binet, C., Lavalley, J-C., Galtayries, A., and Spoken, R., *Phys. Chem. Chem. Phys.*, 1999, vol. 1, p. 5717.
15. Binet, C. and Daturi, M., *Catal. Today*, 2001, vol. 70, p. 155.
16. Bianci, D., Chafik, T., Khalfallah, M., and Teichner, S.J., *Appl. Catal., A*, 1995, vol. 123, p. 89.

17. Li, C., Sakata, Y., Arai, T., Domen, K., Maruya, K., and Onishi, T., *J. Chem. Soc., Faraday Trans. 1*, 1989, vol. 85, no. 4, p. 920.
18. Lu-Cun Wang, Qian Liu, Miao Chen, Yong-Mei Liu, Yong Cao, He-Yong He, and Kang-Nian Fan, *J. Phys. Chem. C*, 2007, vol. 111, p. 16549.
19. Shinkarenko, V.G., *Cand. Sci. (Chem.) Dissertation*, Novosibirsk: Inst. of Catalysis, 1978.
20. Wei-Ping Dow, Yu-Piao Wang, and Ta-Jen Huang, *J. Catal.*, 1996, vol. 160, p. 155.
21. Kuznetsova, T.G. and Sadykov, V.A., *Kinet. Katal.*, 2008, vol. 49, no. 6, p. 886 [*Kinet. Catal.* (Engl. Transl.), vol. 49, no. 6, p. 840].
22. Yao, C.-Z, Wang, L.-C., Liu, Y.-M., Wu, G.-S., Cao, Y., Dai, W.-L., He, H.-Y., and Fan, K.-N., *Appl. Catal., A*, 2006, vol. 297, p. 151.
23. Bensitel, M., Moravek, V., Lamotte, J., Saur, O., and Lavalley, J.-C., *Spectrochim. Acta, Part A*, 1987, vol. 12, p. 1487.
24. Jung, K.T. and Bell, A.T., *Top. Catal.*, 2002, vol. 20, nos. 1–4, p. 97.
25. Ouyang, F. and Yao, S., *J. Phys. Chem. B*, 2000, vol. 104, p. 11 253.
26. Davydov, A.A., *IK-spektroskopiya v khimii poverkhnosti okislov* (IR Spectroscopy Applied to the Chemistry of Oxide Surfaces), Novosibirsk: Nauka, 1984.
27. Burcham, L.J. and Wachs, I.E., *Catal. Today*, 1999, vol. 49, p. 467.
28. Sambeth, J.E., Centeno, M.A., Paul, A., Briand, L.E., Thomas, H.J., and Odriozola, J.A., *J. Mol. Catal. A: Chem.*, 2000, vol. 161, p. 89.
29. Busca, G., *Catal. Today*, 1996, vol. 27, p. 457.
30. Fisher, I.A. and Bell, A.T., *J. Catal.*, 1998, vol. 178, p. 153.
31. Matyshak, V.A., Berezina, L.A., Sil'chenkova, O.N., Tret'yakov, V.F., Lin, G.I., and Rozovskii, A.Ya., *Kinet. Katal.*, 2009, vol. 50, no. 1, p. 120 [*Kinet. Catal.* (Engl. Transl.), vol. 50, no. 1, p. 111].
32. Matyshak, V.A., Berezina, L.A., Sil'chenkova, O.N., Tret'yakov, V.F., Lin, G.I., and Rozovskii, A.Ya., *Kinet. Katal.*, 2009, vol. 50, no. 2, p. 270 [*Kinet. Catal.* (Engl. Transl.), vol. 50, no. 2, p. 255].
33. Choi, Y. and Stenger, H.G., *Appl. Catal., B*, 2002, vol. 38, p. 259.
34. Rozovskii, A.Ya., *Kinet. Katal.*, 2003, vol. 44, no. 3, p. 391 [*Kinet. Catal.* (Engl. Transl.), vol. 44, no. 3, p. 360].
35. Rozovskii, A.Ya. and Lin, G.I., *Teoreticheskie osnovy sinteza metanola* (Theoretical Principles of Methanol Synthesis), Moscow: Khimiya, 1990.